Hydrogen Storage

DOI: 10.1002/anie.200604306

Assembly of Metal–Organic Frameworks (MOFs) Based on Indium-Trimer Building Blocks: A Porous MOF with soc Topology and High Hydrogen Storage**

*Yunling Liu, Jarrod F. Eubank, Amy J. Cairns, Juergen Eckert, Victor Ch. Kravtsov, Ryan Luebke, and Mohamed Eddaoudi**

The potential of the molecular-building-block (MBB) approach for the assembly and development of functional solid-state porous materials has already been recognized.[1] This approach offers a prospective avenue toward the design and construction of novel materials; that is, desired properties can be incorporated at the design stage. These properties are required to address the myriad technological challenges that face us, including hydrogen storage for fuel applications. In metal–ligand directed assembly, the MBB approach has been adopted for the synthesis of functional metal–organic assemblies (MOAs), which range from discrete (metal–organic polyhedra) to 3D (metal–organic frameworks (MOFs)). Accordingly, various applications, including nonlinear optics (NLO), magnetism, catalysis, and gas storage, were revealed for MOFs.[2,3] These MOFs have proven exceptional owing to their facile tunability (alteration in pore size and functionality), a feature dependent on the rigidity, modularity, and control of the MBBs. Therefore, prior to the assembly process, it is essential that the MBBs possess certain attributes for the construction of targeted structures: each must be rigid, impart the desired directionality, and possess the necessary shape and geometry for that structure.

Organic chemistry would seem to offer a vast repertoire to be employed as MBBs, because organic molecules can be designed to contain these features. Nevertheless, organic-molecule-based MBBs with high connectivity are not common, and their assembly into crystalline porous organic frameworks remains a challenge.[4] As such, alternative routes have been pursued combining organic MBBs and inorganic MBBs derived from metal–ligand coordination. Unlike organic MBBs, which are selected already possessing the desired features, typically inorganic MBBs are formed in situ. As a result, reaction conditions to generate a specific inorganic MBB consistently in situ are vital; once established, desired MOAs can be designed and (potentially) assembled by judicious choice of organic ligands. It is clear that continuous development and isolation of novel MBBs will eventually facilitate the rational construction of targeted functional MOAs, an example of design versus serendipity.

Strategies based on the MBB approach have already shown promise toward the design and construction of MOAs, and, accordingly, some basic guidelines have been derived:[1] 1) It is essential that the desired inorganic building blocks can be targeted. 2) The organic linker must have specific functionalities that give rise to the desired shape, geometry, and rigidity upon coordination. 3) Reaction conditions must introduce the ability to generate crystalline materials, a result that is vital for structural analysis and correlations between structure and building units. 4) It is accepted that the assembly of simple building blocks, in the absence of any altering agent such as a template or structure directing agent (SDA), will lead to the construction of the default structure relative to those specific building blocks, and, therefore, design methods that impart directionality and rigidity are invaluable.

Our research group has utilized these guidelines to target porous MOAs based on rigid and directional single indium-centered tetrahedral building units (TBUs) and having non-default topologies.[5] As MOAs from p-block metals are rare and our previous studies with indium involve rigid building blocks based on the single-metal ions and organic chelating moieties with N,O-donors, we began to explore conditions to synthesize other potential indium-based building blocks, specifically those derived from metal carboxylates. Metal–carboxylate clusters often generate a rigid node with fixed

[*] Dr. Y. Liu, J. F. Eubank, A. J. Cairns, Dr. V. C. Kravtsov, R. Luebke, Prof. Dr. M. Eddaoudi
Department of Chemistry
University of South Florida
4202 East Fowler Avenue (CHE 205), Tampa, FL 33620 (USA)
Fax: (+1) 813-974-3203
E-mail: eddaoudi@cas.usf.edu
Dr. Y. Liu
State Key Laboratory of Inorganic Synthesis and Preparative Chemistry, Jilin University
Changchun 130012 (P.R. China)
Dr. J. Eckert
Materials Research Laboratory
University of California, Santa Barbara
Santa Barbara, CA 93106-5121 (USA)
and
LANSCE-LC, Los Alamos National Laboratory
Los Alamos, NM 87545 (USA)
Dr. V. C. Kravtsov
Institute of Applied Physics of Academy of Sciences of Moldova
Academy str. 5, MD2028 Chisinau (Moldova)

[**] We gratefully acknowledge the financial support of the National Science Foundation (DMR 0548117) and NASA (NGA3-2751), and we would like to express our gratitude to Ray Ziegler and Nicolas de Souza for their assistance with the neutron scattering experiments at IPNS, ANL (operated by the UChicago Argonne, LLC for the US DOE under contract DE-AC02-06CH11357). soc = square–octahedron.[19,20]

Supporting information for this article (PXRD and X-ray crystallographic data) is available on the WWW under http://www.angewandte.org or from the author.

geometry involving multiple metal–oxygen coordination bonds which induce the stability of the node and subsequently enhance the thermal stability and overall rigidity of the framework.[1d–f,6] To date, most contributions have focused primarily on the use of transition-metal-based clusters, such as, but not limited to, dimeric MBBs ($[M_2(CO_2)_4]$ square paddlewheels[7]) and tetrameric MBBs ($[Zn_4O(CO_2)_6]$ clusters[8]).

Initial experiments with indium and linear ditopic carboxylate-based organic linkers, not surprisingly, led to the assembly of single-metal-ion-based TBUs ($[In(CO_2)_4]$) into metal–organic frameworks (MOFs) having diamond-like topology, the default arrangement for tetrahedral nodes.[9] However, under similar reaction conditions, the use of angular organic linkers, such as 1,3-benzenedicarboxylic acid (120°), consistently led to the in situ formation of a novel oxygen-centered indium–carboxylate trimer molecular building block (TMBB), $[In_3O(CO_2)_6]$.

Note that oxo-bridged trimers with the formula $[M_3O(O_2CR)_6L_3]^{n+}$ are common in transition-metal coordination chemistry and are structurally well-established with over 389 structures in the Cambridge Structure Database (CSD; August, 2006).[10] However, 3D MOF structures based on the assembly of TMBBs are still scarce.[11] Only recently have Férey and co-workers reported routes to synthesize porous metal–carboxylate structures from TMBBs, where the metal–acetate trimer acts as a precursor.[12]

Our approach is to extend this type of TMBB to contain p-block elements, such as indium. Although serendipity lead to the formation of this unprecedented cluster, a new avenue has been opened to derive and generate novel extended structures based on the $[In_3O(CO_2)_6]$ TMBB.[13] Herein, we report the synthesis and structure of two MOFs based on the novel oxo-bridged trinuclear indium–carboxylate clusters, one having a cubic structure similar to MIL-59[11d] with a CaB_6 topology and the other exhibiting an unprecedented soc topology (soc = square–octahedron).

Reaction between 1,3-benzenedicarboxylic acid (1,3-H_2BDC) and $In(NO_3)_3{\cdot}2H_2O$ in a *N*,*N*-dimethylformamide (DMF)/CH_3CN solution in the presence of imidazole yields a homogeneous microcrystalline material.[14] The as-synthesized compound was characterized and formulated by elemental microanalysis and single-crystal X-ray diffraction studies as $[In_3O(C_8O_4H_4)_3(H_2O)_{1.5}(C_3N_2H_3)(C_3N_2H_4)_{0.5}]{\cdot}DMF{\cdot}0.5(CH_3CN)$ (**1**).[15] The purity of **1** was confirmed by similarities between its simulated and experimental powder X-ray diffraction (PXRD). The cubic structure of **1** (Figure 1) is built from trimers of corner-sharing octahedrally coordinated indium centers joined by the bent 1,3-BDC organic linkers. The trimers contain three indium-centered octahedra that share one central μ_3-oxo anion located on a threefold axis, which leads to three In-(μ_3-O)-In angles of 120°. Crystallographic analysis shows that the apical positions of the indium ions in the trimer building unit are statistically occupied by water molecules and by deprotonated and neutral imidazole molecules. Each trimer unit is linked by six separate ditopic organic linkers to build up the 3D structure. The framework exhibits similar cuboidal cages to those in MIL-59, and is isostructural to MIL-59 (Figure 1).

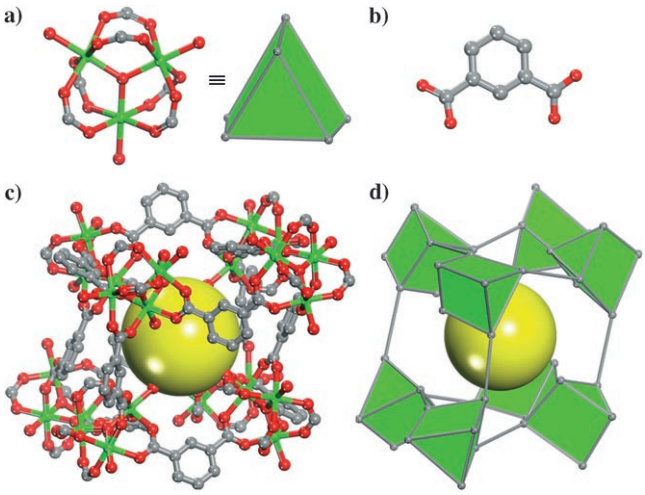

Figure 1. X-ray crystal structure of **1**: a) the oxygen-centered indium–carboxylate TMBB, $[In_3O(CO_2)_6]$, which can be viewed as a 6-connected node having trigonal-prismatic geometry, b) the organic linker, 1,3-benzenedicarboxylate (1,3-BDC), and c) ball-and-stick and d) polyhedral representations of the cuboidal cage of **1**. In green, C gray, O red; the cavity size is indicated by the large yellow spheres. Hydrogen atoms, axial coordinating ligands, and solvent molecules are omitted for clarity.

Similar reaction conditions as for **1** in the presence of piperazine and 3,3′,5,5′-azobenzenetetracarboxylic acid[16,17] as the organic linker give orange polyhedral crystals formulated as $[In_3O(C_{16}N_2O_8H_6)_{1.5}(H_2O)_3](H_2O)_3(NO_3)$ (**2**) by elemental microanalysis and single-crystal X-ray diffraction studies.[18] The crystallographic analysis of **2** revealed that its structure contains similar indium trimer building blocks. The trimers contain three $\{InO_5(H_2O)\}$ octahedra sharing one central μ_3-oxo anion. In each octahedron, the apical position is occupied by a terminal water molecule. Each trimer unit is linked by six separate organic linkers to produce a novel 3D structure. To better understand the framework topology, the components of **2** can be simplified as 4-connected rectangular planar nodes (organic linker) and 6-connected nodes (indium trimeric building units), as seen in Figure 2 a,b. The assembly of these two types of nodes results in the generation of a 3D network having the soc topology[19,20] (Figure 2 d). In the crystal structure of **2** (Figure 2 c), each indium atom is trivalent, yielding an overall cationic framework (+1 per formula unit) that is balanced by $[NO_3]^-$ ions. The disordered $[NO_3]^-$ ions occupy statistically two positions on the threefold axis with equal probability. Therefore, a total of four $[NO_3]^-$ ions reside in each nanometer-scale carcerand-like capsule of **2**, and are not able to escape owing to steric hindrance (window dimensions: 7.651 Å × 5.946 Å, point to point and not including van der Waals radii). Other interesting structural features of **2** are its two types of infinite channels. The first type is hydrophilic, because the water molecules coordinated to the indium centers are pointed inside these channels. Guest water molecules occupy the remaining free volume in these channels and form hydrogen bonds with coordinated water molecules. The second type of channels, with approximately 1-nm diameter, is guest-free in the as-synthesized **2**.[21]

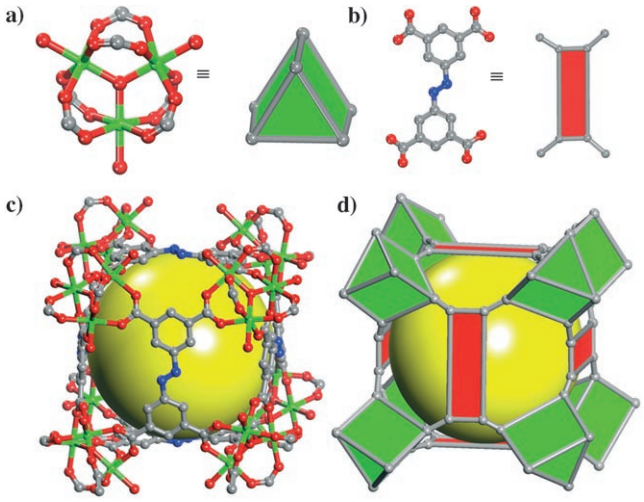

Figure 2. X-ray crystal structure of **2**: a) the oxygen-centered indium–carboxylate TMBB, $[In_3O(CO_2)_6(H_2O)_3]$, which can be viewed as a 6-connected node having trigonal-prismatic geometry, b) the organic linker, 3,3′,5,5′-azobenzenetetracarboxylate, which can be viewed as a 4-connected node having rectangular-planar geometry, and c) ball-and-stick and d) polyhedral representations of the cuboidal cage of **2**. In green, C gray, N blue, O red; the cavity size is indicated by the large yellow spheres). Hydrogen atoms, water molecules, and $[NO_3]^-$ ions are omitted for clarity.

The total solvent-accessible volumes for **1** and **2** were determined by summing voxels more than 1.2 Å away from the framework using PLATON software. They were estimated to be 18.9% (the coordinated imidazolate ligands were not omitted in this calculation) and 57.2%, respectively. The N_2 adsorption/desorption study for **2** revealed a reversible type I isotherm with no hysteresis, characteristic of a microporous material with homogeneous pores (Figure 3a). The estimated Langmuir surface area and pore volume for **2** are 1417 $m^2 g^{-1}$ and 0.50 $cm^3 g^{-1}$, respectively.

Owing to the interesting structural and functional features of **2**, that is, the narrow pores with higher and localized charge density, we explored the H_2 uptake on **2** and found that it can store high amounts, up to 2.61% at 78 K and 1.2 atm (Figure 3b). The isosteric heat of adsorption, up to 1.8% loading of H_2 per sorbent weight, was calculated to be $q = 6.5$ kJ mol^{-1} (Figure 3c), a value appreciably larger than that observed for carbon porous materials[22] and similar to the values for MOFs.[23] The constancy of the heat of adsorption for uptake up to 1.8% per weight, the maximum amount sorbed at 87 K and 1.2 atm, is indicative of the homogeneity of the sorption sites for **2** up to this experimental loading (ca. 70% of the full loading of 2.61% H_2 at 78 K and 1.2 atm). This result reveals the potential influence of open metal sites, framework charges, and pore dimensions on the energetics of sorbed H_2 molecules in MOFs. The importance of open metal sites on H_2 sorption has, in fact, been confirmed for several MOFs,[24] as well as the impact of electrostatic interactions of the sorbed H_2 within the pores of charged frameworks (zeolites).[25] The large amounts of H_2 adsorbed on **2** (2.61%) suggest a higher density of H_2 within the pores (0.05 g cm^{-3}) when compared to values for other MOFs.[3a]

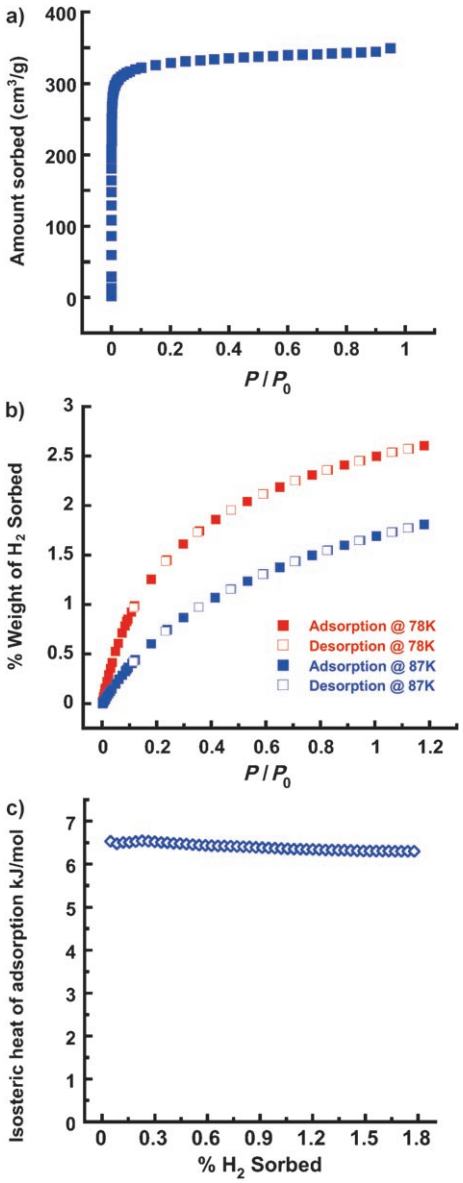

Figure 3. a) Nitrogen sorption isotherm on **2** at 78 K. b) Hydrogen sorption isotherms on **2** at 78 and 87 K. c) Isosteric heat of adsorption for **2**.

This higher population of H_2 molecules in the pores approaches a liquid-like state (0.0708 g cm^{-3} at 20 K) at atmospheric pressures and higher temperatures (78 K), probably driven by the narrow pores (1 nm) that result in an overlap of potential energy fields of the pore walls combined with the residential charge density within the pores.

To obtain a better understanding of the sorption sites within **2**, inelastic neutron scattering (INS) was used to study the respective interactions of molecular H_2 with the framework. The INS spectra of the rotational transitions of the adsorbed H_2 molecules were obtained at 15 K on **2** by using in situ loading of H_2 at doses equivalent to one, two, three, five, and seven H_2 molecules per indium atom. The spectra shown in Figure 4 are of a similar quality to those obtained for hydrogen in several other MOFs,[24] and thereby indicate the presence of reasonably well-defined binding sites. As in

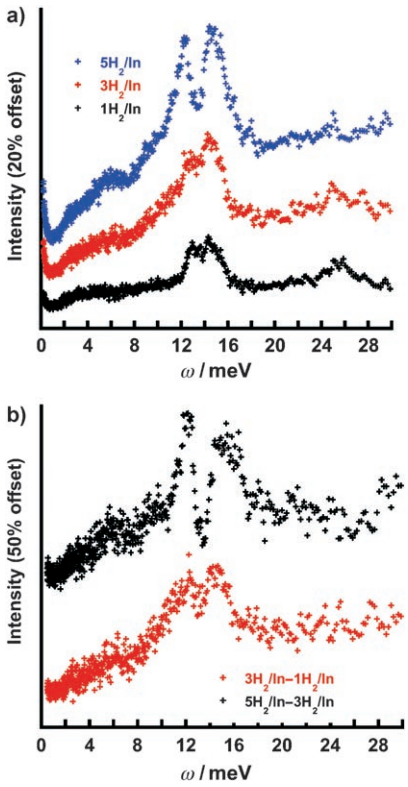

Figure 4. a) Inelastic neutron scattering spectra of **2** obtained at 15 K on the quasielastic neutron spectrometer (QENS) at the intense pulsed neutron source (IPNS) at Argonne National Laboratory (ANL) for loadings of 1, 3, and 5 H_2/In and b) difference spectra. New peaks appearing at the highest loading become evident in the difference spectra in (b).

previous studies, we find that even at the lowest loading of 1 H_2/In, multiple sites are occupied, despite the fact that the interaction of H_2 at the vacant indium coordination sites (created by removal of the apical water molecules upon dehydration) ought to be the strongest.[24] This finding is in accord with the relatively constant value of isosteric heats of adsorption at loadings below 1.8 % H_2 uptake (Figure 3c).

To assign the considerable number of observed peaks, it is necessary to use a model for the rotational potential experienced by the H_2 molecule, detailed in the Supporting Information. At the 1 H_2/In loading, several peaks are observed, which validates the concurrent occupation of multiple sites at this relatively low uptake. The three most intense bands may be assigned as 0–1 and 0–2 transitions for weakly bound H_2 as listed in the Supporting Information, Table S1. According to our model, the well-defined peak at about 25.5 meV is likely to be associated with the vacant indium site. The fact that the assignment of the rotational transitions for H_2 at this site can be made based on our model suggests that H_2 is physisorbed, not coordinated, to the exposed metal site, which is in contrast to previous observations.[26] We can make inferences about the nature of the weak binding sites from the dependence of the INS spectra on H_2 loading. The principal observed effect of extra loading up to 3 H_2/In is an increased intensity of the strong bands around 12.8 and 14 meV, that is, the filling of more of the non-indium sites, which supports our assignments and indicates predominant occupation of most of the vacant indium sites at 1 H_2/In. Since we have identified the open-indium sites, the identity of the remaining sites can be associated with the organic components of the framework, that is, carboxylate, azo, and phenyl moieties. Note that at loadings higher than 5 H_2/In (H_2 uptake greater than 1.8 % and close to the maximum H_2 uptake of 2.61 % at 78 K and 1.2 atm) some additional binding sites become available (Supporting Information, Table S1) with *stronger* interactions (lower energies compared to the sites occupied by H_2 at reduced loadings of 1 and 3 H_2/In). This situation, which is apparent in the difference spectra (Figure 4b), is in marked contrast to previous observations in MOFs, where sites with weak guest–host interactions are typically populated at the highest loadings.[23]

This unique INS finding at the higher loading of 5 H_2/In, potentially, can be correlated to the unique structural features of **2**, namely the presence of isolated nanometer-scale carcerand-like capsules, which anchor nitrate ions, and which are strictly accessible through the two main channels by very restricted windows (Supporting Information, Figure S4). Accordingly, we believe that the isolated cages containing nitrate ions are not accessible at lower loadings owing to the higher sorption kinetic-energy diffusion barrier associated with the restricted entrance. This barrier is pronounced at the low experimental temperature of 78 K. We believe that at 78 K and at lower loadings below 3 H_2/In, primarily the channels are occupied, and that at higher loadings, close to 5 H_2/In, the isolated cages become accessible owing to increased local concentration (pressure) of H_2 near the cavity entrances, which allows the limiting sorption kinetic energy diffusion barrier to be overcome. Accordingly, access to such narrow cavities which enclose high local charge density permits the exposure of H_2 molecules to stronger sorption sites, as supported by the INS studies at higher loadings. These observations are completely in accord with the elevated H_2 density (0.05 $g\,cm^{-3}$) observed in the pores of **2** at 78 K.[27]

The structural analysis of **2**, combined with the INS and sorption studies, suggests that narrower pores (<1 nm) and/or higher localized charge densities can be suitable for higher uptake of H_2. Therefore, we believe that MOFs possessing these characteristics, combined with the modularity of their construction that allows higher surface areas to be obtained, will permit the attainment of the US Department of Energy (DOE) target for H_2 uptake in the near future.

Currently, we are exploring several avenues to increase the uptake, including the ability to design and synthesize porous MOFs combining high surface area, higher charge densities, and narrow pores around 1 nm, similar to those obtained in **2**. Also, the ability to generate trimeric clusters from several lighter metals offers great potential to synthesize an $[Al_3O(CO_2)_6]$ trimer based soc MOF, which will theoretically adsorb similar amounts of H_2 per unit volume and, most importantly, higher uptake per weight unit (estimated to be 3.0 %).

Received: October 20, 2006
Revised: January 18, 2007
Published online: March 27, 2007

Keywords: hydrogen storage · indium · metal–organic frameworks · molecular building blocks · porous materials

[1] a) M. Fujita, M. Tominaga, A. Hori, B. Therrien, *Acc. Chem. Res.* **2005**, *38*, 369–378; b) O. M. Yaghi, M. O'Keeffe, N. W. Ockwig, H. K. Chae, M. Eddaoudi, J. Kim, *Nature* **2003**, *423*, 705–714; c) L. R. MacGillivray, J. L. Atwood, *Nature* **1997**, *389*, 469–472; d) A. K. Cheetham, G. Férey, T. Loiseau, *Angew. Chem.* **1999**, *111*, 3466–3492; *Angew. Chem. Int. Ed.* **1999**, *38*, 3268–3292; e) B. Moulton, M. J. Zaworotko, *Chem. Rev.* **2001**, *101*, 1629–1658; f) S. R. Seidel, P. J. Stang, *Acc. Chem. Res.* **2002**, *35*, 972–983.

[2] a) G. Férey, C. Mellot-Draznieks, C. Serre, F. Millange, *Acc. Chem. Res.* **2005**, *38*, 217–225; b) C. D. Wu, A. Hu, L. Zhang, W. Lin, *J. Am. Chem. Soc.* **2005**, *127*, 8940–8941; c) S. Kitagawa, R. Kitaura, S. Noro, *Angew. Chem.* **2004**, *116*, 2388–2430; *Angew. Chem. Int. Ed.* **2004**, *43*, 2334–2375; d) O. Kahn, *Acc. Chem. Res.* **2000**, *33*, 647–657; e) O. R. Evans, W. Lin, *Acc. Chem. Res.* **2002**, *35*, 511–512; f) H. R. Moon, J. H. Kim, M. P. Suh, *Angew. Chem.* **2005**, *117*, 1287–1291; *Angew. Chem. Int. Ed.* **2005**, *44*, 1261–1265.

[3] a) N. L. Rosi, J. Eckert, M. Eddaoudi, D. T. Vodak, J. Kim, M. O'Keeffe, O. M. Yaghi, *Science* **2003**, *300*, 1127–1129; b) S. S. Kaye, J. R. Long, *J. Am. Chem. Soc.* **2005**, *127*, 6506–6507; c) G. Férey, M. Latroche, C. Serre, F. Millange, T. Loiseau, A. Percheron-Guegan, *Chem. Commun.* **2003**, 2976–2977; d) D. N. Dybtsev, H. Chun, K. Kim, *Angew. Chem.* **2004**, *116*, 5143–5146; *Angew. Chem. Int. Ed.* **2004**, *43*, 5033–5036; e) X. Zhao, B. Xiao, A. J. Fletcher, K. M. Thoms, D. Bradshaw, M. J. Rosseinsky, *Science* **2004**, *306*, 1012–1015.

[4] A. P. Cote, A. I. Benin, N. W. Ockwig, M. O'Keeffe, A. J. Matzger, O. M. Yaghi, *Science* **2005**, *310*, 1166–1170.

[5] a) Y. Liu, V. Ch. Kravtsov, R. Larsen, M. Eddaoudi, *Chem. Commun.* **2006**, 1488–1490; b) Y. Liu, V. Ch. Kravtsov, D. A. Beauchamp, J. F. Eubank, M. Eddaoudi, *J. Am. Chem. Soc.* **2005**, *127*, 7266–7267; c) Y. Liu, V. Ch. Kravtsov, R. D. Walsh, P. Poddar, H. Srikanth, M. Eddaoudi, *Chem. Commun.* **2004**, 2806–2807; d) J. A. Brant, Y. Liu, D. F. Sava, D. Beauchamp, M. Eddaoudi, *J. Mol. Struct.* **2006**, *796*, 160–164.

[6] M. Eddaoudi, D. B. Moler, H. Li, B. Chen, T. M. Reineke, M. O'Keeffe, O. M. Yaghi, *Acc. Chem. Res.* **2001**, *34*, 319–330.

[7] a) B. Moulton, J. Lu, R. Hajndl, S. Hariharan, M. J. Zaworotko, *Angew. Chem.* **2002**, *114*, 2945–2948; *Angew. Chem. Int. Ed.* **2002**, *41*, 2821–2824; b) M. Eddaoudi, J. Kim, D. Vodak, A. Sudik, J. Wachter, M. O'Keeffe, O. M. Yaghi, *Proc. Natl. Acad. Sci. USA* **2002**, *99*, 4900–4904; c) O. M. Yaghi, C. E. Davis, G. Li, H. Li, *J. Am. Chem. Soc.* **1997**, *119*, 2861–2868.

[8] H. Li, M. Eddaoudi, M. O'Keeffe, O. M. Yaghi, *Nature* **1999**, *402*, 276–279.

[9] Y. Liu, M. Eddaoudi, unpublished results.

[10] F. H. Allen, *Acta Crystallogr. Sect. B* **2002**, *58*, 380–388.

[11] a) O. M. Yaghi, R. Jernigan, H. Li, C. E. Davis, T. L. Groy, *J. Chem. Soc. Dalton Trans.* **1997**, 2383–2384; b) H. Li, C. E. Davis, T. L. Groy, D. G. Kelley, O. M. Yaghi, *J. Am. Chem. Soc.* **1998**, *120*, 2186–2187; c) J. S. Seo, D. Whang, H. Lee, S. I. Jun, J. Oh, Y. Jin, K. Kim, *Nature* **2000**, *404*, 982–986; d) K. Barthelet, D. Riou, G. Férey, *Chem. Commun.* **2002**, 1492–1493; e) G. Férey, C. Serre, C. Mellot-Draznieks, F. Millange, S. Surblé, J. Dutour, I. Margiolaki, *Angew. Chem.* **2004**, *116*, 6456–6461; *Angew. Chem. Int. Ed.* **2004**, *43*, 6296–6301; f) A. C. Sudik, A. P. Cote, O. M. Yaghi, *Inorg. Chem.* **2005**, *44*, 2998–3000; g) G. Férey, C. Mellot-Draznieks, C. Serre, F. Millange, J. Dutour, S. Surblé, I. Margiolaki, *Science* **2005**, *309*, 2040–2042.

[12] C. Serre, F. Millange, S. Surblé, G. Férey, *Angew. Chem.* **2004**, *116*, 6445–6449; *Angew. Chem. Int. Ed.* **2004**, *43*, 6285–6289.

[13] It should be noted that the indium trimer now has been reported by one other group, but only after compounds **1** and **2** had been synthesized and fully characterized. C. Volkringer; T. Loiseau, *Mater. Res. Bull.* **2006**, *41*, 948–954.

[14] Preparation of **1**: 1,3-H_2BDC, (30.0 mg, 0.174 mmol), $In(NO_3)_3{\cdot}2H_2O$ (30.0 mg, 0.087 mmol), DMF (1 mL), CH_3CN (1 mL), imidazole (0.2 mL, 0.90 M in DMF), and HNO_3 (0.2 mL, 2.7 M in DMF) were added to a vial, and the solution was heated to 85 °C for 12 h and then at 100 °C for 20 h. Colorless cubic crystals were collected and air-dried (23.5 mg, 75% yield). The as-synthesized material is insoluble in H_2O and common organic solvents. Elemental analysis calcd (%) for **1**, $C_{32.5}H_{28.5}N_{4.5}O_{15.5}In_3$: C 36.33, H 2.67, N 5.87; found: C 36.15, H 2.82, N 5.92.

[15] Crystallographic data of **1**: $C_{32.5}H_{28.5}In_3N_{4.5}O_{15.5}$, $M_r = 1074.56$, cubic, $Pa\bar{3}$, $a = 19.5514(9)$ Å, $V = 7473.7(6)$ Å^3, $Z = 8$, $\rho_{calcd} = 1.910\ g\,cm^{-3}$, $2\theta_{max} = 54.98°$ ($-10 \le h \le 25$, $-15 \le k \le 16$, $-25 \le l \le 23$), $T = 100$ K, 20484 measured reflections, $R_1 = 0.0520$, $wR_2 = 0.1319$ for 2436 reflections ($I > 2\sigma(I)$), and $R_1 = 0.0649$, $wR_2 = 0.1387$ for 2870 independent reflections (all data) and 177 parameters, GOF = 1.016. Data were collected on a Bruker SMART-APEX CCD diffractometer using $Mo_{K\alpha}$ radiation ($\lambda = 0.71073$ Å), operating in the ω and φ scan mode and corrected for Lorentz and polarization effects. The SADABS program was used for absorption correction. The structures were solved by direct methods and the structure solutions and refinements were based on $|F^2|$. All non-hydrogen atoms were refined with anisotropic displacement parameters, except the atoms of disordered fragments, which were refined isotropically. Hydrogen atoms were placed in calculated positions and given isotropic U values 20% higher than the atom to which they are bonded. All crystallographic calculations were conducted with the SHELXTL software suite. CCDC-624027 (**1**) and CCDC-624028 (**2**) contain the supplementary crystallographic data for this paper. These data can be obtained free of charge from The Cambridge Crystallographic Data Centre via www.ccdc.cam.ac.uk/data_request/cif.

[16] Synthesis of 3,3′,5,5′-azobenzenetetracarboxylic acid: S. Wang, X. Wang, L. Li, R. C. Advincula, *J. Org. Chem.* **2004**, *69*, 9073–9084.

[17] Preparation of **2**: 3,3′,5,5′-azobenzenetetracarboxylic acid[16] (16.0 mg, 0.044 mmol), $In(NO_3)_3{\cdot}2H_2O$ (22.0 mg, 0.065 mmol), DMF (1 mL), CH_3CN (0.5 mL), piperazine (0.1 mL, 0.4 M in DMF), and HNO_3 (0.28 mL, 2.7 M in DMF) were added to a vial, and the solution was heated to 85 °C for 12 h. Orange-colored polyhedral crystals were collected and air-dried (16.6 mg, 72% yield). The as-synthesized material is insoluble in H_2O and common organic solvents. Elemental analysis calcd (%) for **2**, $C_{24}H_{21}N_4O_{22}In_3$: C 27.15, H 1.99, N 5.28; found: C 27.32, H 2.51, N 5.18.

[18] Crystallographic data of **2**: $C_{24}H_{21}In_3N_4O_{22}$, $M_r = 1061.91$, cubic, $P\bar{4}3n$, $a = 22.4567(11)$ Å, $V = 11325.0(10)$ Å^3, $Z = 8$, $\rho_{calcd} = 1.246\ g\,cm^{-3}$, $2\theta_{max} = 50.02°$ ($-15 \le h \le 15$, $0 \le k \le 18$, $1 \le l \le 26$), $T = 100$ K, 3352 measured reflections, $R_1 = 0.0680$, $wR_2 = 0.1760$ for 1499 reflections ($I > 2\sigma(I)$), and $R_1 = 0.0855$, $wR_2 = 0.1844$ for 1819 independent reflections (all data) and 156 parameters, GOF = 1.039.

[19] M. O'Keeffe, M. Eddaoudi, H. Li, T. Reineke, O. M. Yaghi, *J. Solid State Chem.* **2000**, *152*, 3–20.

[20] M. O'Keeffe, Reticular Chemistry Structure Resource, http://rcsr.anu.edu.au/.

[21] G. Yang, S. C. Sevov, *J. Am. Chem. Soc.* **1999**, *121*, 8389–8390.

[22] a) C. N. Brown, T. Yildirim, D. A. Neumann, M. J. Heben, T. Gennett, A. C. Dillon, J. L. Alleman, J. E. Fischer, *Chem. Phys. Lett.* **2000**, *329*, 311–316; b) Y. Ren, D. L. Price, *Appl. Phys. Lett.* **2001**, *79*, 3684–3686.

[23] a) J. L. C. Rowsell, O. M. Yaghi, *J. Am. Chem. Soc.* **2006**, *128*, 1304 – 1315; b) J. Y. Lee, L. Pan, S. P. Kelly, J. Jagiello, T. J. Emge, J. Li, *Adv. Mater.* **2005**, *17*, 2703 – 2706; c) J. Y. Lee, J. Li, J. Jagiello, *J. Solid State Chem.* **2005**, *178*, 2527 – 2532.

[24] J. L. Rowsell, J. Eckert, O. M. Yaghi, *J. Am. Chem. Soc.* **2005**, *127*, 14904 – 14910.

[25] a) J. M. Nicol, J. Eckert, J. Howard, *J. Phys. Chem.* **1988**, *92*, 7117 – 7121; b) J. Eckert, J. M. Nicol, J. Howard, F. R. Trouw, *J. Phys. Chem.* **1996**, *100*, 10646 – 10651.

[26] P. M. Forster, J. Eckert, J. Chang, S. Park, G. Férey, A. K. Cheetham, *J. Am. Chem. Soc.* **2003**, *125*, 1309 – 1312.

[27] We note that these new transitions at lower frequencies (that is, higher barriers to rotation) at high loadings cannot be the result of intermolecular interactions between H_2 molecules, as these interactions are comparatively rather weak: H_2 molecules in the bulk solid are essentially freely rotating. See, for example, I. Silvera, *Rev. Mod. Phys.* **1980**, *52*, 393.

